Indian Journal of Pure & Applied Physics
Vol. 53, April 2015, pp. 247-256

External electric field effect on the nonlinear optical properties of a laser dressed donor impurity in a GaAs spherical quantum dot confined at the center of a $Ga_{1-x}Al_xAs$ cylindrical nano-wire

Gh Safarpour[1,*], M A Izadi[2], M Novzari[2] & E Niknam[2]

[1]Young Researchers and Elite Club, Shiraz Branch, Islamic Azad University, Shiraz, Iran

[2]Young Researchers and Elite Club, Zarghan Branch, Islamic Azad University, Zarghan, Iran

*E-mail: safarpour.ghasem@gmail.com

Received 5 February 2014; revised 14 July 2014; accepted 12 February 2015

Linear and third order nonlinear optical absorption coefficients and refractive index changes of an on-center donor impurity in a spherical GaAs quantum dot which is located at the center of a cylindrical $Ga_{1-x}Al_xAs$ nano-wire, have been investigated under the simultaneous effect of electric field and laser radiation. The linear and third order nonlinear optical properties are calculated based on optical 1-2, 2-3 and 1-3 transitions by means of the compact density-matrix approach. The energy eigenvalues and corresponding wave functions are calculated using finite difference approximation and reliability of calculated wave functions is checked by computing orthogonality. It is shown that optical spectrum shifts towards lower and higher energies for 1-2 transition and shifts towards lower energies for 2-3 and 1-3 transitions as the electric field strength increases. The presence of laser field shifts absorption spectrum towards lower energies. In the absence of electric and laser field, the magnitude of absorption coefficient and refractive index changes increase in transitions between higher levels. Simultaneous presence of both electric field and laser radiation has great effect on magnitude of absorption coefficients and refractive index changes. The saturation in optical spectrum can be adjusted by electric field and laser radiation.

Keywords: Nonlinear optics, Laser dressed donor impurity, External electric field, Spherical quantum dot, Nano-wire

1 Introduction

Since the beginning of quantum theory, the investigation of electronic and optical properties of confined quantum systems has been an interesting subject. Among all confined systems, quantum dots (QDs) have attracted great attention due to the motion of charge carriers which is confined in three dimensions[1-3]. Additionally, developments in precise engineering enable us to fabricate zero-dimensional QDs embedded into one-dimensional nano-wires[4,5]. The one-dimensional geometry of the nano-wire has an important benefit which allows researchers to incorporate QDs in this active region. As a result of the possible applications, researchers have used this structure as a single photon source[6,7], calculated electronic structure of quantum dots is embedded into nano-wires[8-10]. The exciton lifetime in individual InAsP QDs which is perfectly positioned on-axis of InP nano-wire[11]. The orientation-dependent optical-polarization properties of single QD in nano-wires have been studied[12].

The effect of impurities on the optical properties of semiconductor QDs has also been studied by researchers. Beside the impurity, the presence of an intense non-resonant laser field has resulted into a number of investigations[13-16]. The simultaneous presence of impurity and laser field causes a laser-dressed Coulomb potential in the system.Therefore, a noticeable change in the magnitude and position of absorption peak is obtained in the presence of an intense laser field.

The effects of external factors such as pressure[17], magnetic field[18] and electric field[19] on nanostructures have been studied. The effect of external electric field on the electronic and optical properties of QDs has been reported by several researchers[20-25]. The understanding of the electric field dependence of optical properties of QDs is important for building efficient optoelectronic devices[26]. These studies show that the presence of electric field has a great effect on the optical properties of the system which depends on the geometrical parameters. For instance Xie *et al*[19]. studied electric field effects on the optical properties of two different geometries (I) disc-like QD in presence of donor impurity (II) a spherical QD in presence of donor or acceptor impurity[27]. The

presence of electric field causes a red shift in absorption spectrum in the presence of donor impurity, a blue shift in presence of acceptor impurity and a decrement in the *ac* magnitude in both cases. Also, Kirak *et al*[21]. investigated the electric field effects on the nonlinear optical properties of a donor impurity in a spherical QD and illustrated that the presence of electric field shifts absorption spectrum to the higher energies (blue shift) and increases magnitude of the ACs, for both 0s-1p and 1p-2d transitions.

Moreover, the studies of optical properties have been extended to transitions between different sub-bands such as 1-2, 2-3 and 3-1 transitions[28], 1-2 and 2-4 transitions[29],1-2, 1-3 and 2-4 transitions[30], 1s-1p, 1p-1d and 1d-1f transitions[31-33]. If we compare reported results by Xie[27] and Kirak *et al*[21]., it is clear that different shifts and different variation of magnitude of absorption coefficient have been reported, whereas both works are related to the spherical QD in presence of the electric field and donor impurity. It is due to different states between which the transitions will occur. The optical properties have been investigated for 1-2, 2-3 and 1-3 transitions in the present paper.

The effects of electric field and laser radiation parameters on the optical properties of a spherical QD located at the center of a cylindrical nano-wire, have been investigated in the present paper.

2 Theory

GaAs spherical QD with radius R_1, located at the center of a $Ga_{1-x}Al_xAs$ cylindrical nano-wire with radius R_2 and height l, has been considered. The origin is taken at the bottom of the nano-wire and the z-axis is defined to be along the nano-wire axis. In the effective mass approximation and in the cylindrical coordinates Hamiltonian of a single particle in presence of an external electric field can be expressed as:

$$H^0(\rho,\phi,z) = -\frac{\hbar^2}{2m^*(\rho,z)} \times\left(\frac{\partial^2}{\partial\rho^2}+\frac{1}{\rho}\frac{\partial}{\partial\rho}+\frac{1}{\rho^2}\frac{\partial^2}{\partial\phi^2}+\frac{\partial^2}{\partial z^2}\right) +V(\rho,z)+eFz \quad \ldots(1)$$

where $m^*(\rho, z)$ is the band edge effective mass, which may vary with position due to the changes in material composition, the electric field is assumed to be in the z-direction with strength F and the electron confining potential, $V(\rho,z)$, is given by:

$$V(\rho,z)=\begin{cases}0 & \sqrt{\rho^2+(z-l/2)^2}<R_1\\ v & \sqrt{\rho^2+(z-l/2)^2}>R_1 \\ & \quad \& \rho\le R_2 \,\&\, 0\le z\le l\end{cases} \quad \ldots(2)$$

where $v=Q_c(E_g^{Ga_{x-x}Al_xAs}-E_g^{GaAs})$, E_g is the band-gap energy and Q_c is the band offset ratio[34]. In the presence of an on-center hydrogenic donor impurity and a laser field with vector potential $\vec{A}(t)=A_0(\cos\Omega t\hat{i}+\sin\Omega t\hat{j})$ the Hamiltonian of the system[35,36] can be rewritten as:

$$H(\rho,\phi,z)=H^0(\rho,\phi,z)-\frac{e^2}{4\pi\varepsilon_r\varepsilon_0} \times\frac{1}{\sqrt{\rho^2+(z-l/2)^2+\alpha_0^{\,2}}} \quad \ldots(3)$$

where $\alpha_0=eA_0/(m^*\Omega)=(8\pi/\Omega c)^2\sqrt{I_\alpha}e/m^*$ is the amplitude of the electron oscillation in the laser field, Ω is laser field frequency, I_α is the laser field intensity and c is speed of light. Three first lower-lying states and corresponding wave functions of the Hamiltonian of Eq. (3) have been found. Since our geometry has axial symmetry, the azimuthal part of the wave functions can be separated as: $F_m(\phi)=\frac{1}{\sqrt{2\pi}}e^{im\phi}$. It is worth pointing out that we just calculate the energy levels with respect to m=0. Therefore, the Schrödinger equation can be rewritten as:

$$\left\{-\frac{\hbar^2}{2m^*(\rho,z)}\left(\frac{\partial^2}{\partial\rho^2}+\frac{1}{\rho}\frac{\partial}{\partial\rho}+\frac{\partial^2}{\partial z^2}\right)+V^{eff}(\rho,z)\right\} \times\Psi(\rho,z)=E\Psi(\rho,z) \quad \ldots(4)$$

where

$$V^{eff}(\rho,z)=V(\rho,z)+eFz -\frac{e^2}{4\pi\varepsilon_r\varepsilon_0}\frac{1}{\sqrt{\rho^2+(z-l/2)^2+\alpha_0^{\,2}}}.$$

The Schrödinger equation is numerically solved by the finite difference (FD) approximation[37-39]. In order to carry out simulation numerically, one needs to

discretize Eq. (4) using FD schemes. First it should to be noted that to avoid achieving a huge coefficient matrix, the non-uniform space discretization is considered along z-coordinate with aspect ratio $\frac{\Delta z_{j+1}}{\Delta z_j}=\frac{z_{j+1}-z_j}{z_j-z_{j-1}}=1.1$. This aspect ratio ensures a sufficient convergence of electronic structure. Additionally, for ρ-coordinate a uniform space discretization is applied. The spatial derivative is approximated by the central FD scheme for all discretized space except on boundaries and given by:

$$\begin{aligned}&\frac{1}{m^*(\rho,z)}\left(\frac{\partial^2}{\partial\rho^2}+\frac{1}{\rho}\frac{\partial}{\partial\rho}+\frac{\partial^2}{\partial z^2}+V^{eff}(\rho,z)\right)\psi^{(in,out)}(\rho,z)\\&\cong\frac{1}{m^*(\rho_i,z_j)\Delta\rho^2}(\psi^{(in,out)}(i+1,j)-2\psi^{(in,out)}(i,j)\\&+\psi^{(in,out)}(i-1,j))+\frac{1}{m^*(\rho_i,z_j)\rho\Delta\rho}(\psi^{(in,out)}(i+1,j)\\&-\psi^{(in,out)}(i,j))+\frac{1}{m^*(\rho_i,z_j)\Delta z_j{}^2}(\psi^{(in,out)}(i,j+1)\\&-2\psi^{(in,out)}(i,j)+\psi^{(in,out)}(i,j-1))\\&+(V^{eff}(i,j))\psi^{(in,out)}(i,j)\end{aligned}\quad\ldots(5)$$

The notation $\psi^{(in,out)}(i,j)\equiv\psi^{(in,out)}(i\Delta\rho,z_j+\Delta z_j)$ ($\Delta\rho$ and Δz_j are spatial spacing) is used in this paper and the superscriptions *"in"* and *"out"* represent the wave functions inside and outside the dot. For discretized space on different boundaries, different FD schemes should to be applied[40] as : (I) for boundary $(\forall\rho,z=0)$ the forward FD scheme is applied (II) for boundary $(\forall\rho,z=l)$ the backward FD scheme is applied (III) for boundary $(\rho=0,\forall z)$ the forward FD scheme is used for ρ-coordinate and the central FD scheme for z-coordinate (IV) for boundary $(\rho=R_2,\forall z)$ the backward FD scheme is used for ρ-coordinate. The Dirichlet boundary condition (i.e., infinite potential barrier) has been imposed at the nano-wire boundaries. The continuity of the wave function and its derivative on the QD boundary $(\sqrt{\rho^2+(z-l/2)^2}=R_1)$ are imposed and considered by appropriate FD schemes.

After determining the electronic structure, the compact-density-matrix approach and the iterative procedure are applied to obtain the analytic formula of the linear and nonlinear optical absorption coefficients(ACs) and refractive index (RI) changes. In low-dimensional systems, the absorption process is defined as an optical transition between an initial state, i, and a final state, f, by absorbing a photon. We consider the system subject to an electromagnetic field, $E(t)=\tilde{E}e^{i\omega t}+c.c$. We assume that the radiation polarized parallel to the unit vector $\hat{u}$. The electronic polarization of the system, $p(t)$, caused by the incident field, $E(t)$, can be written[41] as:

$$p(t)=\varepsilon_0\chi(\omega)\tilde{E}e^{i\omega t}+\varepsilon_0\chi(-\omega)\tilde{E}e^{-i\omega t}\quad\ldots(6)$$

where ε_0 is the free-space electrical permittivity and $\chi(\omega)$ is the Fourier component of the susceptibility of the system. Using the usual iterative procedure[42], the linear and third order nonlinear optical susceptibilities can be obtained. The absorption coefficient $\{\alpha(I,\omega)\}$ is related to the susceptibility as $\alpha(\omega)=\omega\sqrt{\frac{\mu}{\varepsilon_r\varepsilon_0}}\,\mathrm{Im}[\varepsilon_0\chi(\omega)]$. Then, neglecting the higher harmonic terms, the analytical form of the linear and third order nonlinear ACs are given by Ref. (42).

$$\alpha^{(1)}(\omega)=\omega\sqrt{\frac{\mu}{\varepsilon_r\varepsilon_0}}\,\frac{\sigma_v\left|M_{fi}\right|^2\hbar\Gamma_{fi}}{(E_{fi}-\hbar\omega)^2+(\hbar\Gamma_{fi})^2}\quad\ldots(7)$$

$$\begin{aligned}\alpha^{(3)}(I,\omega)=&-\omega\sqrt{\frac{\mu}{\varepsilon_r\varepsilon_0}}\left(\frac{I}{2\varepsilon_0 n_r c}\right)\\&\times\frac{\sigma_v\left|M_{fi}\right|^2\hbar\Gamma_{fi}}{[(E_{fi}-\hbar\omega)^2+(\hbar\Gamma_{fi})^2]^2}\\&\times\left\{4\left|M_{fi}\right|^2-\frac{(M_{ff}-M_{ii})^2[3E_{fi}^2-4E_{fi}\hbar\omega+\hbar^2(\omega^2-\Gamma_{fi}{}^2)]}{E_{fi}{}^2+(\hbar\Gamma_{fi})^2}\right\}\end{aligned}\quad\ldots(8)$$

In Eqs (7 and 8), σ_v is the carrier density, c is the velocity of light in free space, μ is the magnetic permeability, $I=2\varepsilon_0 n_r c\left|E\right|^2$ is the intensity of electromagnetic field, $M_{fi}=\left|<f\left|e\vec{z}.\hat{u}\right|i>\right|$ are the dipole moment matrix elements and $E_{fi}=E_f-E_i$ is

the energy difference between fth and ith states. $\hbar\Gamma_{fi}$ are damping terms associated with the lifetime of the electrons due to intersub-band scattering. $\Gamma_{fi}\,(f \neq i)$ are called as the relaxation rate between fth and ith states[27]. These quantities are related to a high extent electron–phonon interaction, and they need to be taken into account[43].

The changes in RI are related to the susceptibility as $\frac{\Delta n(\omega)}{n_r} = \mathrm{Re}\left(\frac{\chi(\omega)}{2n_r^{\,2}}\right)$. Using this relation, the analytical expressions for the linear and third order nonlinear RI changes, imply the evaluation of the following expressions which are given[42] by :

$$\frac{\Delta n^1(\omega)}{n_r} = \frac{1}{2n_r^{\,2}\varepsilon_0}\frac{\sigma_v \left|M_{fi}\right|^2 (E_{fi}-\hbar\omega)}{(E_{fi}-\hbar\omega)^2+(\hbar\Gamma_{fi})^2} \qquad \ldots(9)$$

$$\begin{aligned}\frac{\Delta n^3(\omega)}{n_r} = &-\frac{\mu c I}{4n_r^{\,3}\varepsilon_0}\frac{\sigma_v \left|M_{fi}\right|^2}{[(E_{fi}-\hbar\omega)^2+(\hbar\Gamma_{fi})^2]^2} \\ &\times\left\{4(E_{fi}-\hbar\omega)\left|M_{fi}\right|^2 - \frac{(M_{ff}-M_{ii})^2}{E_{fi}^{\,2}+(\hbar\Gamma_{fi})^2}\right. \\ &\times[(E_{fi}-\hbar\omega)(E_{fi}(E_{fi1}-\hbar\omega)-(\hbar\Gamma_{fi})^2)] \\ &\left.-(\hbar\Gamma_{fi})^2(2E_{fi}-\hbar\omega)]\right\} \qquad \ldots(10)\end{aligned}$$

where $n_r = \sqrt{\varepsilon_r}$ denotes the static component of RI. The total AC and RI changes can be written as:

$$\alpha(I,\omega) = \alpha^{(1)}(\omega) + \alpha^{(3)}(I,\omega) \qquad \ldots(11)$$

$$\frac{\Delta n(\omega)}{n_r} = \frac{\Delta n^1(\omega)}{n_r} + \frac{\Delta n^3(\omega)}{n_r} \qquad \ldots(12)$$

3 Numerical Results and Discussion

The effects of external electric field and laser field have been studied on the linear and third order nonlinear ACs and RI changes of a GaAs spherical quantum dot which is located at the center of a $Ga_{1-x}Al_xAs$ cylindrical nano-wire. The energy eigenvalues and corresponding wave functions are numerically calculated using FD approximation. The parameters used in the present work are reported[30,31,34] in Table 1. For simplicity, we assume the same relaxation time for all intersubband transitions[31].

In all numerical calculations, the validity of method should to be confirmed. One way to check the accuracy of the produced wave functions is to test the orthogonality between states which are exactly orthogonal[37]. For solving an eigenvalue problem with FD approximation, the first step is to discretize the space and apply different FD schemes[38]. This discrete approximation leads to finite-dimensional matrix representation. In presented method for a geometry with parameters R_1=6 nm, R_2=20 nm and l=400 nm, the dimension of the matrix is set to be 6545×6545. This matrix dimension is suitable for a processor with 22 GByte RAM. In Table 2, the absolute values of orthogonalities between three first lower-lying states, $|\langle 1|2\rangle|$, $|\langle 2|3\rangle|$, $|\langle 1|3\rangle|$, are presented in presence and absence of external electric field and laser radiation. It is clear that calculated wave functions are as reliable as expected. In the rest part of this paper, optical properties are calculated for 1-2, 2-3 and 1-3 transitions and dot radius, nano-wire radius, nano-wire height and aluminium concentration are set to be R_1=6 nm, R_2=20 nm and L=400 nm and x=0.3, respectively.

Figure 1 shows the linear, third order nonlinear and total optical ACs of the system as a function of the incident photon energy,in absence of laser field and for three different values of electric field strength. The following points are deduced from Fig. 1, for all transitions, the maximum value of total AC corresponds to the threshold photon energy, i.e.,

Table 1 — Values of parameters used in our calculations

Parameters	Values
$m^*Ga_{1-x}Al_xAs/m_0$	$0.0632+0.856+0.0231x^2$
$E_g^{Ga_xAl_{1-x}As}$	$1.424+1.510x+x(1-x)(0.127-1.310x)$
Q_c	0.7
T_{fi}	0.14 ps
R_1	6 nm
R_2	20 nm
l	400 nm

Table 2 — Absolute value of orthogonality between three first lower-lying states ($|\langle 1|2\rangle|$, $|\langle 2|3\rangle|$ and $|\langle 1|3\rangle|$ in presence and absence of electric and laser fields

	$\lvert\langle 1\rvert 2\rangle\rvert\times10^{-11}$	$\lvert\langle 2\rvert 3\rangle\rvert\times10^{-11}$	$\lvert\langle 1\rvert 3\rangle\rvert\times10^{-11}$
F=0 KV/cm, α_0=0 nm	3.2316	1.7267	2.9603
F=15 KV/cm, α_0=0 nm	18.6537	17.00	56.7040
F=0 KV/cm, α_0=20 nm	0.1901	0.1120	0.3842
F=15 KV/cm, α_0=20 nm	11.0723	11.3328	11.0723

$E_{ji} \approx h\nu$. Additionally, for all transitions the linear AC is positive whereas the third order nonlinear term is negative. Therefore, the total AC is reduced by taking into account the nonlinear contribution[31]. For 1-2 transition, the inter sub-band absorption spectrum shows red shift up to a certain value of electric field (F=15 KV/cm), by further increasing of the electric field the absorption spectrum shifts towards higher energies (blue shift). It is due to the variation of energy difference between ground and first excited states, E_{21}. By increasing the electric field strength, E_{21} decreases, reaches a minimum value and then increases. The red or blue shift in absorption spectrum has been individually reported by several researchers[18,19,27,44] but the presence of both blue and red shifts is an intrinsic property of the considered geometry in this paper. For 2-3 and 1-3 transitions, the peak values of ACs shift towards lower energies (red shift) as the electric field increases which is a direct consequence of decreasing effect of electric field on the E_{32} and E_{31}. For 2-3 and 1-3 transitions, the ACs are smaller for stronger electric field. For 1-2 transition and for small strengths of electric field (F<15 KV/cm), we can see that both the linear and third order nonlinear ACs decrease with increasing electric field. Therefore, it leads to a decrement in total AC. For large values of the electric field (F=15 KV/cm), a reverse behaviour is observed. For this region $|M_{21}|$ and E_{21} are increased by increasing the strength of electric field but the energy difference between ground and first excited states is a dominant factor and causes a decrement in absolute value of the third order AC. Therefore, total AC increases as the electric field strength increases.

In order to investigate the effect of the laser field on the optical properties, the linear, third order nonlinear and total ACs are plotted in Fig. 2 as a function of the photon energy in absence of electric field. It is obvious that for all transitions a red shift appears in absorption spectrum with respect to the laser field. The physical origin of this behaviour is that by increasing the laser field the effective dressed Coulomb potential decreases, which in turn decreases the energy difference between different states between which the transition will occur. In absence and presence of laser filed, both ground and first excited states are localized inside the dot but the absence of laser field (i.e. stronger Coulomb potential) causes more localization of the ground and first excited states which is equivalent to a reduction

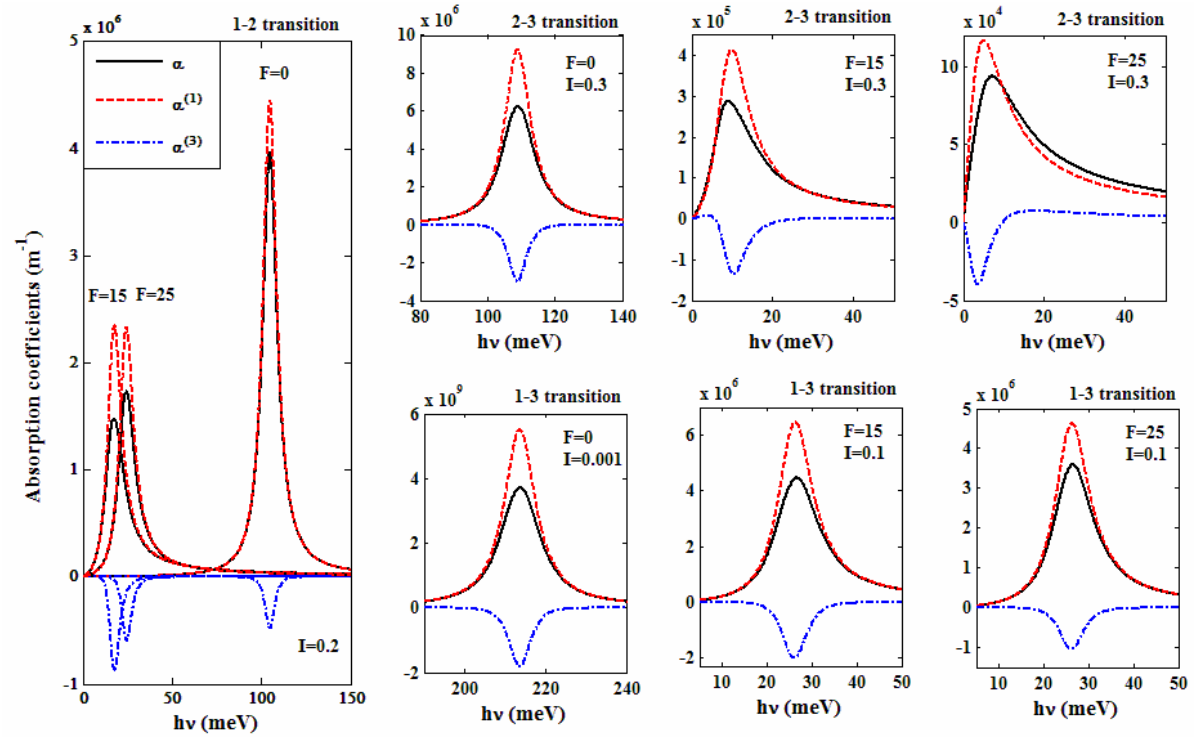

Fig. 1 — Linear, third order nonlinear and total optical ACs for 1-2, 2-3 and 1-3 transitions as a function of the incident photon energy for three different values of strength of electric field

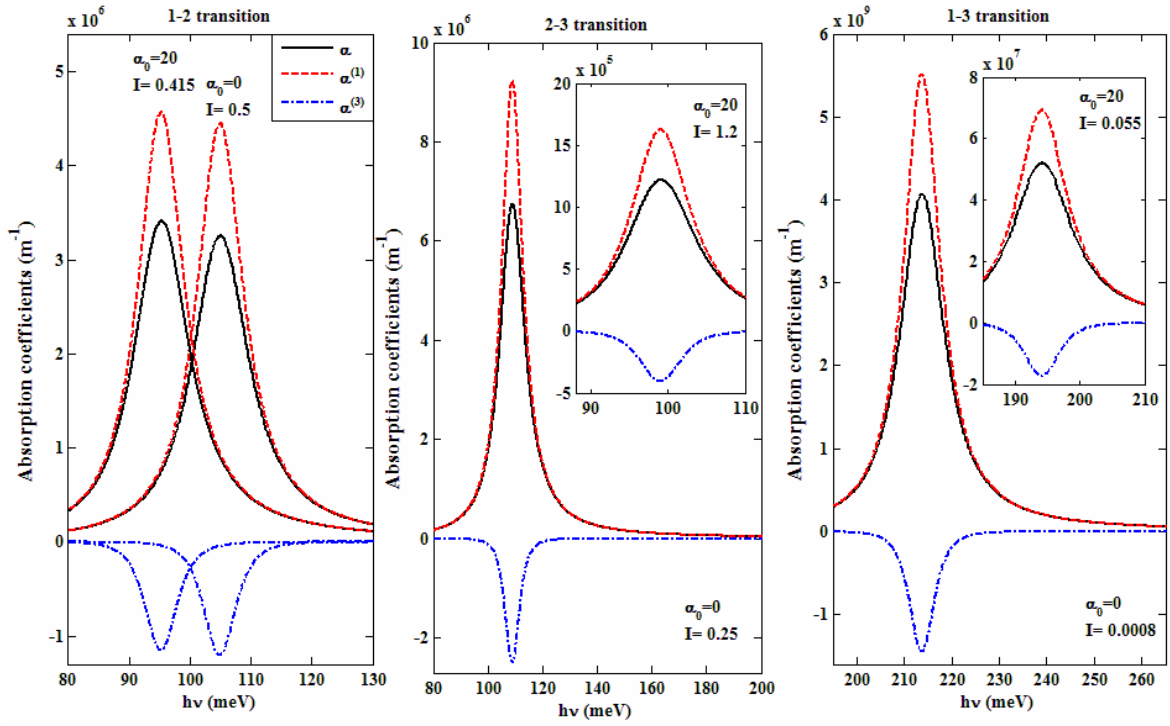

Fig. 2 — Linear, third order nonlinear and total optical ACs for 1-2, 2-3 and 1-3 transitions as a function of the incident photon energy for two different values of laser field

in the overlap of the wave functions. This behaviour leads to a reduction in the linear AC. On the other hand, in absence of the laser field, the second excited state is also mostly confined in the QD but the expectation value of the position vector for this state is larger than it for ground or first excited state. Hence, by increasing the laser field, the dressed Coulomb potential decreases, therefore, the geometric confinement of the electron in the second excited state decreases,so, it can penetrate into the potential barriers easily. This penetration modifies the sub-band dispersion relations and causes a reduction in the overlap wave function between ground and second excited states or first and second excited states[28,45]. Therefore, the magnitude of the absorption coefficient becomes smaller by increasing the laser field for 1-3 and 2-3 transitions.

The RI changes are other important parameter in investigation of optical properties. In Fig. 3, the linear, third-order nonlinear and total RI changes have been plotted as a function of the incident photon energy for different values of electric field strength. Additionally, in Fig. 4 the same quantities are plotted for two different values of laser field, α_0=0, 20 nm. As can be seen from Figs 3 and 4, RI curves have been plotted for different incident optical intensities for 1-2, 2-3 and 1-3 transitions. The reason of choosing different incident optical intensities is shown in Fig. 5. From Figs 3 and 4, it is clear that each RI curves has two extreme values. The region between these extreme values is called anomalous dispersion region and is defined as absorption band, since the photon is strongly absorbed[33]. Also, for each RI curve the threshold energy is where the RI curve intersects the horizontal axis. As can be seen, by increasing the strength of the electric field or laser field the threshold energies shift towards lower and/or higher energies. The physical reason of this behaviour is the same as has been shown in Figs 1 and 2. For 2-3 and 1-3 transitions, RI changes increase the electric field or laser field decreases, especially for 1-3 transition where the variations in RI curves are noticeably large. It is because of that the square of dipole moment matrix element is dramatically large for 1-3 transition. For 1-2 transition, RI changes increase as the laser field increases (see Fig. 4) and increase up to a certain value of electric field and then decrease as the electric field increases (see Fig. 3).

It is noticed from Eqs (7-10) that the linear AC and RI changes do not depend on photon intensity but the

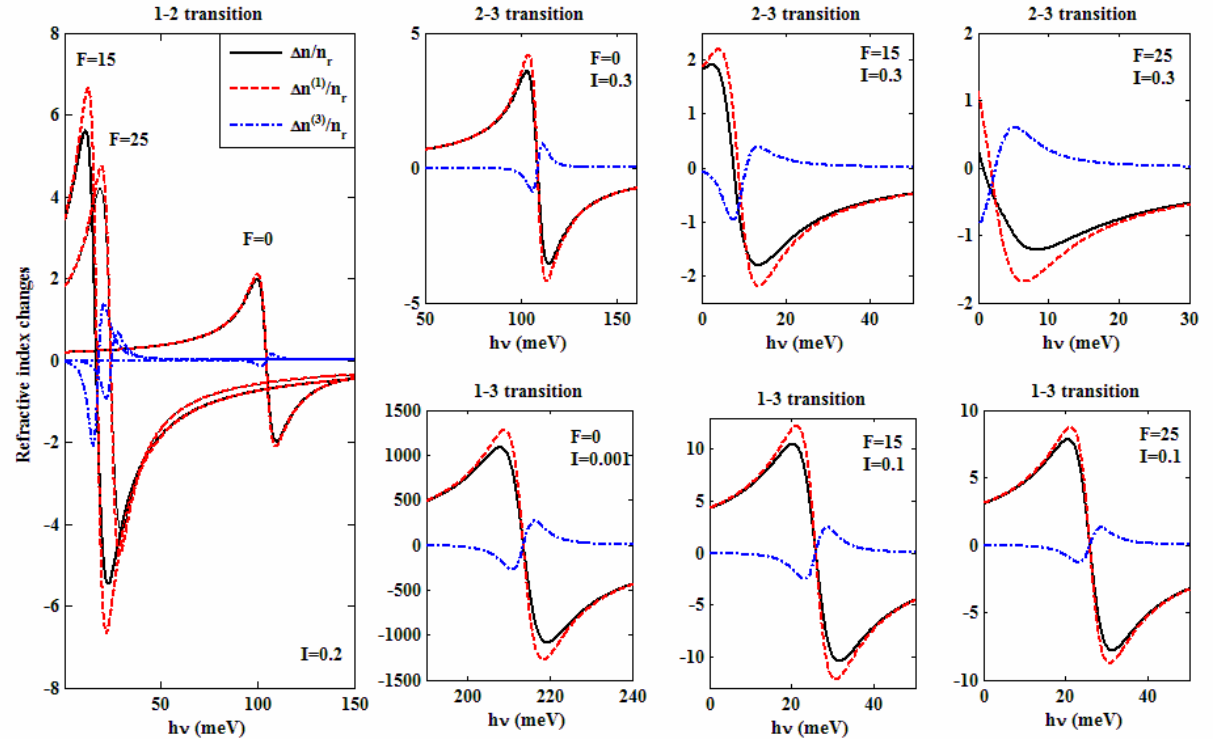

Fig. 3 — Linear, third order nonlinear and total optical RI changes for 1-2, 2-3 and 1-3 transitions as a function of the incident photon energy for three different values of strength of electric field

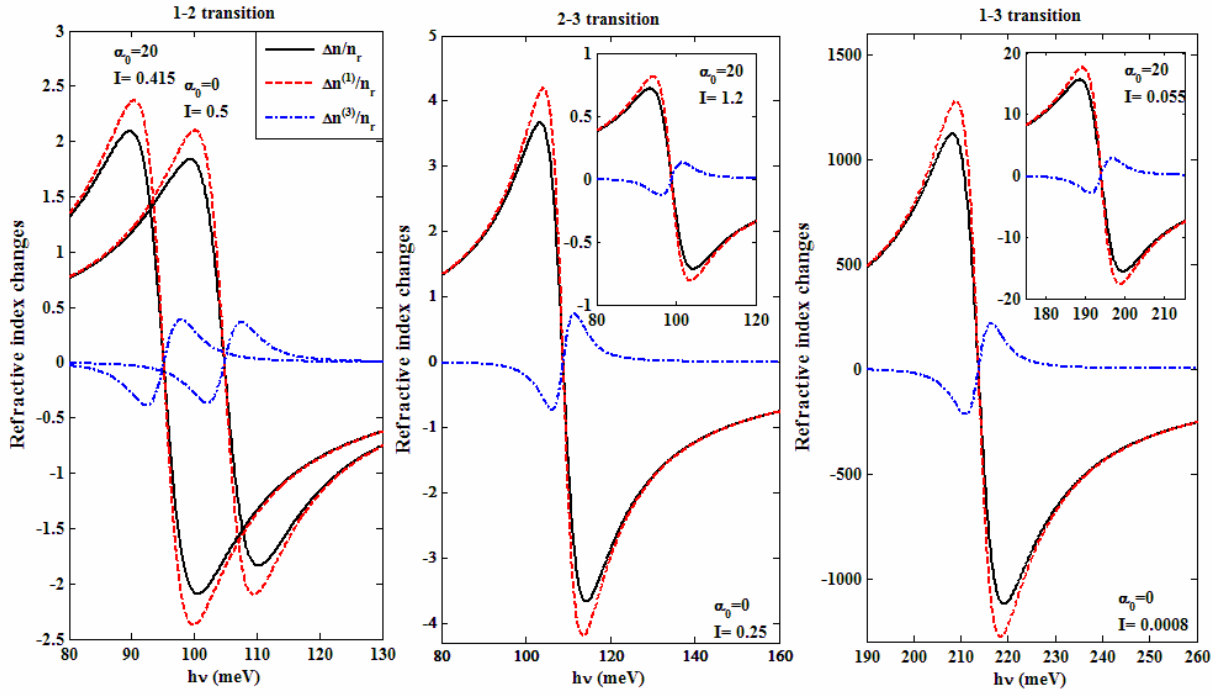

Fig. 4 — Linear, third order nonlinear and total optical RI changes for 1-2, 2-3 and 1-3 transitions as a function of the incident photon energy for two different values of laser field

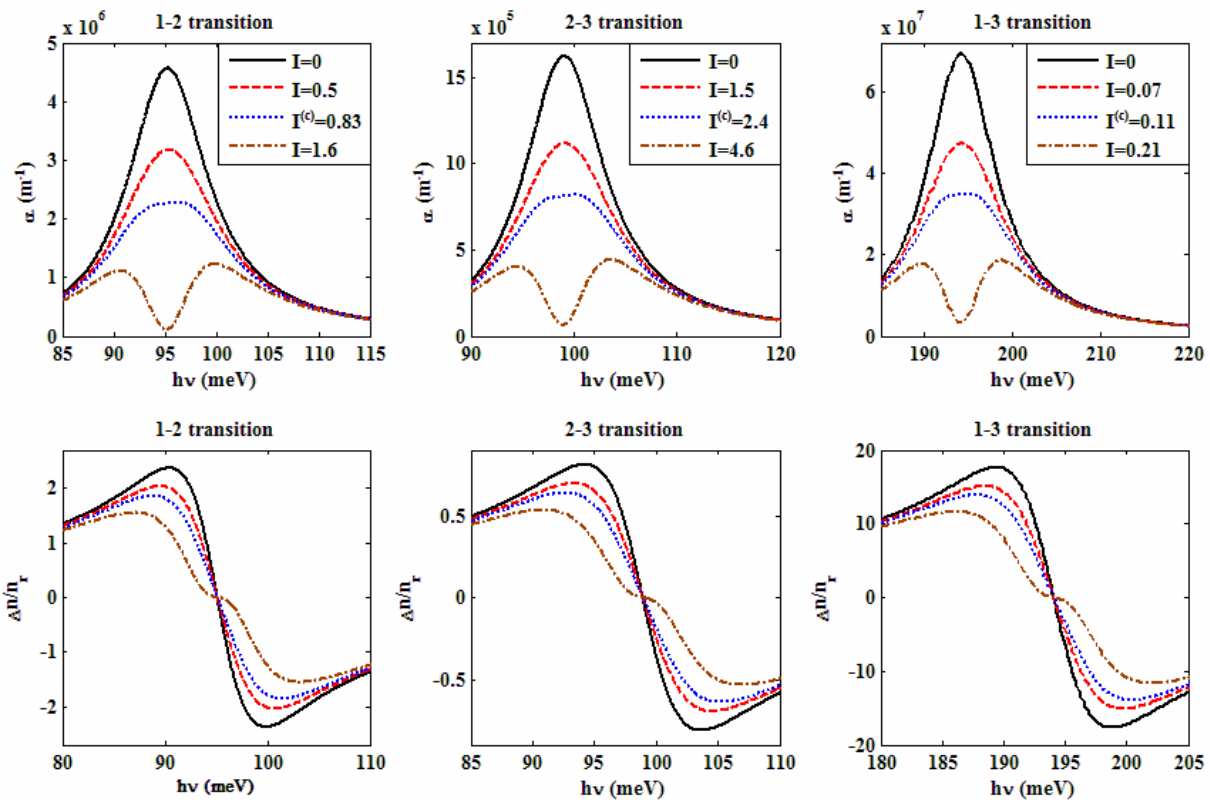

Fig. 5 — Total optical AC and RI changes for 1-2, 2-3 and 1-3 transitions as a function of the incident photon energy for four different values of incident optical intensity, in absence of electric field and laser radiation

third order AC and RI changes vary with photon intensity. Therefore, to see how the photon intensity affects the optical properties of the system, in Fig. 5 the total optical AC and RI changes have been presented as a function of the incident photon energy in the absence of electric field and laser radiation for five different values of the incident optical intensity (I). From Fig. 5, it is clear that maximum value of AC decreases with increasing incident optical intensity, and the absorption is strongly bleached at sufficiently high incident optical intensities. When I exceeds a critical value, $I^{(c)}$, which indicates saturation, the nonlinear term causes a collapse at the center of the total absorption peak and splits it into two peaks[32]. Moreover, the critical I values depend on the transitions and are equal to $I^{(c)}$=1 MW/cm^2, $I^{(c)}$=0.5 MW/cm^2 and $I^{(c)}$=0.0016 MW/cm^2 for 1-2, 2-3 and 1-3 transitions. To illustrate the effects of laser field and electric field on the critical I values, they are calculated in the presence of laser and electric fields for 1-2, 2-3 and 1-3 transitions. Computed results are equal to $I^{(c)}$=0.83 MW/cm^2, $I^{(c)}$=2.4 MW/cm^2 and $I^{(c)}$=0.11 MW/cm^2 for F=0 KV/cm, α_0=20 nm and are equal to $I^{(c)}$=1.26 MW/cm^2, $I^{(c)}$=0.7 MW/cm^2 and $I^{(c)}$=0.15 MW/cm^2 for F=15 KV/cm, α_0=0 nm. It is clear that critical I values strongly depend on the presence and absence of electric and laser fields as well as on the states between which the transition will occur. We can explain this behaviour as follows: Increasing the electric field results in an increase in overlap of the wave functions for all transitions, whereas, increasing laser field leads to an increment (a decrement) in overlap of the wave functions for 1-2 transition (2-3 and 1-3 transitions). On the other hand, due to the large overlap of the wave functions the linear absorption becomes bigger; hence, in this case the nonlinear absorption coefficient rapidly increases with the optical intensity which leading to a significant absorption bleaching[30].Additionally, for $I \cong 0$ the nonlinear changes in RI is equal to zero. As the incident optical intensity increases, the absolute value of nonlinear term increases, in other words, the amplitude of the total RI changes decreases which is equivalent to the wider AC. Furthermore, this means

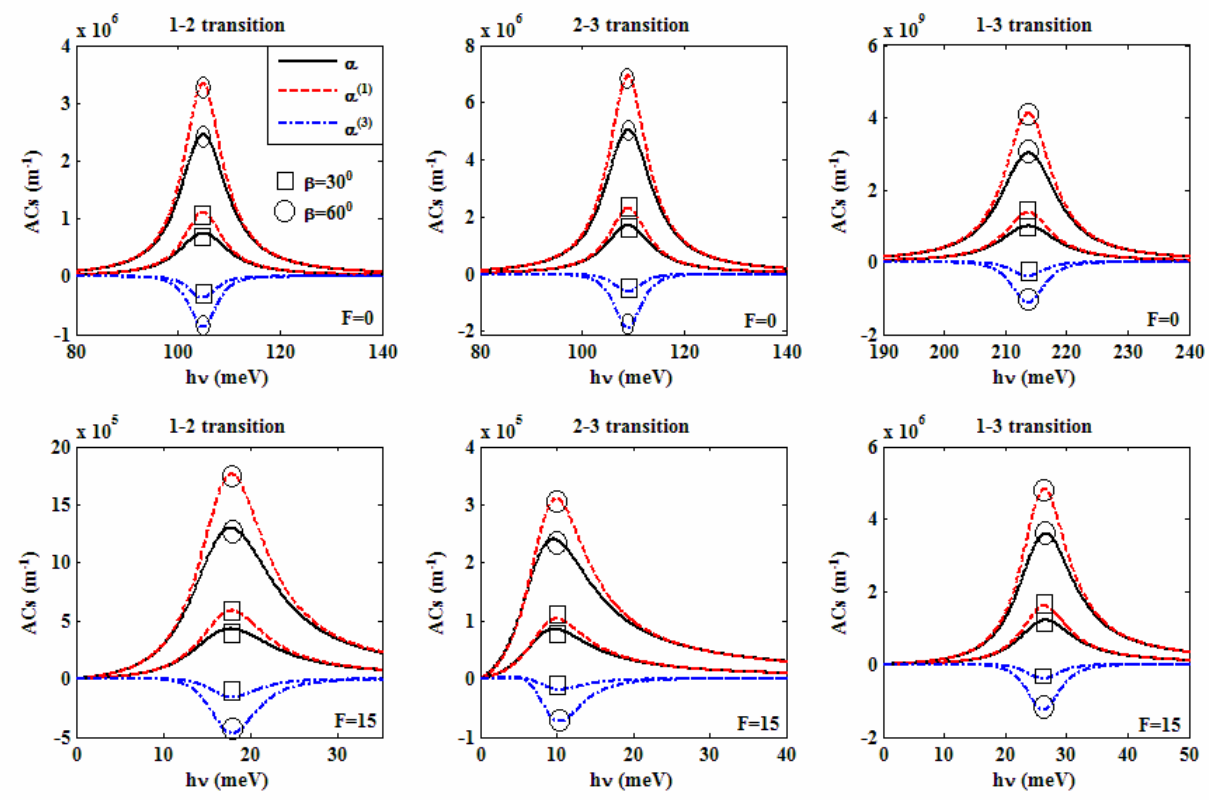

Fig. 6 — Linear, third order nonlinear and total optical ACs for 1-2, 2-3 and 1-3 transitions as a function of the incident photon energy for two different values of β and different strengths of electric field

that by increasing the incident optical intensity the anomalous dispersion region increases. Therefore, to study the optical properties, the nonlinear term should be taken into account, especially when the incident optical intensity is comparatively strong. Due to these facts in Figs 1-4 the ACs and RI changes have been presented for 1-2, 2-3 and 1-3 transitions with different incident optical intensity for each transition.

To investigate the effect of orientation of incident electromagnetic field upon the optical properties, the linear, third order nonlinear and total AC have been presented as a function of the photon energy for two representative β in Fig. 6, where β is the angle between radiation unit vector and z-axis. Fig. 6 shows the effect of β on the ACs in presence and absence of external electric field for 1-2, 2-3 and 1-3 transitions. By comparing Fig. 1 with Fig. 6, it is evident that ACs are inversely proportional to β. We also noticed that smaller β leads to higher and sharper peaks in the ACs. On the other hand, we also find that the ACs peaks appear at the same photon energy when β increases. This indicates no blue or red shift in absorption spectrum due to confinement strength and does not change with respect to β.

4 Conclusions

In conclusion, the linear, third order nonlinear and total ACs and RI changes of a GaAs spherical QD which is located at the center of a $Ga_{1-x}Al_xAs$ cylindrical nano-wire, have been investigated. The energy eigenvalues and wave functions are calculated by FD approximation. The accuracy of applied method is tested by evaluating the orthogonality between different states. It is shown that produced solutions by the applied method are of high accuracy. Optical ACs and RI changes are calculated for 1-2, 2-3 and 1-3in the presence of electric field and laser radiation using density matrix formalism. Our results show that presence of electric field causes a red shift in ACs for 2-3 and 1-3 transitions and both blue and red shift for 1-2 transition. The laser radiation leads to a dressed Coulomb potential, and so decreases the energy difference between states which transition occurs. Additionally, the magnitude of total AC

reduces by increasing the electric field and/or laser field for 2-3 and 1-3 transitions whereas for 1-2 transition the magnitude of total AC decreases, reaches a minimum value and then increases by increasing electric field. Moreover, the total optical absorption is strongly affected by the incident optical intensity and critical *I* value depends on the electric field, laser radiation and energy states between which transitions occur. These effects can be useful for the design of optoelectronic devices.

References

1 Madan Shikha, *Phys Scr*, 82 (2010) 045702.
2 Ahadi M A, Vahdani M R K & Alipour E, *Phys Scr*, 86 (2012) 035701.
3 R Khordad, *Solid State Sci*, 19 (2013) 63.
4 Shorubalko I, Leturcq R, Pfund A, Tyndall D, Krischek R, Schon S & Ensslin K, *Nano Lett*, 8 (2008) 382.
5 Borgstrom M T, Zwiller V, Muller E & Imamoglu A, *Nano Lett,* 5 (2005) 1439.
6 Reimer M E, Kouwen M P van, Barkelid M, Hocevar M, Weert M H M van, Algra R E, Bakkers E P A M, Bjork M T, Schmid H, Riel H, Kouwenhoven L P & Zwiller V, *J Nanophoton*, 5 (2011) 053502.
7 Claudon J, Bleuse J, N S Malik, M Bazin, P Jaffrennou, N Gregersen, C Sauvan, P Lalanne & J M Gerard, *Nat Photonics*, 4 (2010) 174.
8 Avramov P V, Fedorov D G, Sorokin P B, Chernozatonskii L A & Ovchinnikov S G, *J Appl Phys*, 104 (2008) 054305.
9 Panev N, Persson A I, Skold N & Samuelson L, *Appl Phys Lett*, 83 (2003) 2238.
10 Safarpour Gh, Barati M, Moradi M, Davatolhagh S & Zamani A, *Superlattices Microstruct*, 52 (2012) 387.
11 Bulgarini G, Reimer M E, Zehender T, Hocevar M, Bakkers Erik P A M, Kouwenhoven Leo P & Zwiller V, *Appl Phys Lett*, 100 (2012) 121106.
12 Maarten H M van Weert, *Small*, 5 (2009) 2134.
13 Prasad V & Silotia P, *Phys Lett A*, 375 (2011) 3910.
14 Saito M, Honma T, Benino Y, Fujiwara T & Komatsu T, *Solid State Sci*, 6 (2004) 1013.
15 Niculescu E C, Eseanu N & Radu A, *Opt Commun*, 294 (2013) 276.
16 Gambhir M, Kumar M, Jha P K & Mohan M, *J Lumin*, 143 (2013) 361.
17 Oubram O, Navarro O, Gaggero-Sager L M, Martinez-Orozco J C & Rodriguez-Vargas I, *Solid State Sci*, 14 (2012) 440.
18 Yesilgul U, Ungan F, Kasapoglu E, Sari H & Sokmen I, *Superlattices Microstruct*, 50 (2011) 400.
19 Xie W & Xie Q, *Physica B*, 404 (2009) 1625.
20 Narayanan M & Peter A John, *Superlattices Microstruct*, 51 (2012) 486.
21 Kirak M, Yilmaz S, Sahin M & Gencaslan M, *J Appl Phys*, 109 (2011) 094309.
22 Sadeghi E, *Superlattices Microstruct*, 50 (2011) 331.
23 Lu L & Xie W, *Phys Scr*, 84 (2011) 025703.
24 Lopez S Y, Mora-Ramos M E & Duque C A, *Solid State Sci*, 12 (2010) 210.
25 Shao S, Guo Kang-Xian, Zhang Zhi-Hai, Li Ning & Peng Chao, *Superlattices Microstruct*, 48 (2010) 541.
26 Heiss D, Kroutvar M, Finley J J & Abstreiter G, *Solid State Commun*, 135 (2005) 591.
27 Xie W, *Physica B*, 405 (2010) 3436.
28 Ozturk E, Sari H & Sokmen I, *Solid State Commun*, 132 (2004) 497.
29 Burileanu L M & Radu A, *Opt Commun*, 284 (2011) 2050.
30 Niculescu E C, Burileanu L M, Radu A & Lupascu A, *J Lumin*, 131 (2011) 1113.
31 Cakir B, Yakar Y, Ozmen A, Sezer M Ozgur & Sahin M, *Superlattices Microstruct*, 47 (2010) 556.
32 Yakar Y, Cakir B & Ozmen A, *Opt Commun*, 283 (2010) 1795.
33 Cakir B, Yakar Y & Ozmen A, *J Lumin*, 132 (2012) 2659.
34 Li E Herbert, *Physica E*, 5 (2000) 215.
35 Lu L, Xie W & Hassanabadi H, *Physica B*, 406 (2011) 4129.
36 Reuben A Merwyn Jasper D, P Nithiananthi & K Jayakumar, *Superlattices Microstruct*, 46 (2009) 710.
37 Cooper J D, Valavanis A, Ikonic Z, Harrison P & Cunningham J E, *J Appl Phys*, 108 (2010) 113109.
38 Sudiarta I Wayan & Geldart D J Wallace, *J Phys A Math Theor*, 40 (2007) 1885.
39 Amiraliyev G M, *A Math Comput*, 162 (2005) 1023.
40 Ozturk E, Sari H & Sokmen I, *Solid State Commun*, 132 (2004) 497.
41 Rezaei G, Vahdani M R K & Vaseghi B, *Physica B*, 406 (2011) 1488.
42 Vahdani M R K & Rezaei G, *Phys Lett A*, 373 (2009) 3079.
43 Mora-Ramos M E, Duque C A, Kasapoglu E, Sari H & Sokmen I, *J Lumin*, 132 (2012) 901.
44 Karimi M J & Rezaei G, *Physica B*, 406 (2011) 4423.
45 Ozturk E, *Eur Phys J B*, 75 (2010) 197.